Available online at www.sciencedirect.com
ScienceDirect
Biochemical and Biophysical Research Communications 350 (2006) 138–146
BBRC
www.elsevier.com/locate/ybbrc

Analysis of neuron-like differentiation of human bone marrow mesenchymal stem cells

Chi Bong Choi [a,d,1], Yun Kyoung Cho [a,b,1], K.V. Bhanu Prakash [a,b], Bo Keun Jee [a,b], Chang Whan Han [b,*], Young-Ki Paik [c], Hwi-Yool Kim [d], Kweon-Haeng Lee [a,e], Namhyun Chung [f], Hyoung Kyun Rha [a]

[a] *Catholic Neuroscience Center, The Catholic University of Korea, Seoul, Republic of Korea*
[b] *Department of Orthopedic Surgery, Daejeon St. Mary's Hospital, College of Medicine, The Catholic University of Korea, 520-2 Daehung-Dong, Jung-Gu, Republic of Korea*
[c] *Yonsei Proteome Research Center, Department of Biochemistry and Bioproducts Research Center, Yonsei University, Seoul, Republic of Korea*
[d] *Department of Veterinary Surgery, College of Veterinary Medicine, Konkuk University, Seoul, Republic of Korea*
[e] *Department of Pharmacology, The Catholic University of Korea, Seoul, Republic of Korea*
[f] *Division of Biotechnology and Genetic Engineering, Korea University, Republic of Korea*

Received 20 August 2006
Available online 14 September 2006

Abstract

The objective of the study was to evaluate differentiation of human bone marrow mesenchymal stem cells into true or pseudo neurons after treating with chemical induction medium in vitro. The morphological changes were assessed using interference contrast microscopy. Immunocytochemistry and Western blotting were performed using neuronal markers. Further evaluation was conducted with proteomic profiling, DNA microarray analysis and the whole-cell patch clamp test. After three hours of treatment with chemical induction medium, nearly three-fourths of the hMSCs changed to cells with a neuronal phenotype. The results of immunocytochemistry and Western blotting showed a high expression of neuronal markers in these cells at 3 h which decreased at 24 h. The proteomics analysis showed no change of proteins related to neuronal differentiation. DNA microarray showed downregulation of neuron related genes. The patch clamp test was unable to demonstrate any similarity to true neurons. Our findings suggest that neuron-like cells derived from chemical induction of hMSCs are not the genuine neurons as they resemble true neurons phenotypically but are different in genotypic and electrophysiological characteristics.

Keywords: Human mesenchymal stem cells; Chemical induced medium; Neuronal markers; Proteomic profiling; DNA microarray analysis; Whole-cell patch clamp test

Human bone marrow mesenchymal stem cells (hMSCs) exhibit many known traits of stem cells. These hMSCs are capable of differentiating into mesenchymal lineages such as nerve cells, in vitro. Many agents such as cytokines, growth factors, neurotrophins, and retinoic acid have been shown to promote neural cell induction and differentiation both in vivo and in vitro, and they have been used for inducing MSCs to differentiate into neural cells [1–3]. Woodbury et al. [4] have reported that both rodent and human MSCs can be rapidly induced (from minutes to a few hours) to differentiate exclusively into neurons (>70%) by simple chemical means in vitro. The majority (80%) of induced MSCs have not only been shown to exhibit a neuronal morphology, but they have also been observed to express several neuronal markers such as: NSE (neuron specific enolase), neurofilament-M, tau, and NeuN [4]. Several studies have shown similar rapid neuronal differentiation from human bone marrow cells [5],

* Corresponding author. Fax: +82 42 2210429.
E-mail address: hancw0523@hotmail.com (C.W. Han).
[1] These authors contributed equally to this work.

0006-291X/$ - see front matter © 2006 Elsevier Inc. All rights reserved.
doi:10.1016/j.bbrc.2006.09.010

adipose-derived stromal cells [6], and adult murine muscle cells using DMSO/BHA (dimethyl sulfoxide/butylated hydroxyanisole) induction protocol [7]. However, other studies have cast doubt on neuronal differentiation of the MSCs using chemical induction medium [8,9]. In this study, we re-evaluated the in vitro differentiation of hMSCs to neuronal cells following cell treatment with a chemical induction medium containing DMSO [4,10]. We performed immunocytochemistry and Western blotting to evaluate neuronal differentiation of the hMSCs using neuronal markers. In addition, we used the information obtained from proteomic profiling, microarray gene expression, and electrophysiology to identify potential genuine neurons, as proteomics study provides a systematic approach for the quantitative and qualitative mapping of the whole proteome [11–13] and also to examine the authenticity of neuron-like cells derived by chemical induction.

In this study, we attempted to determine whether there was genuine or pseudo-neuronal cell change following chemical neuronal differentiation of hMSCs.

Materials and methods

Research protocol. The research protocol was reviewed and approved by the Human Ethical Care Committee (ECC) at Daejeon's St. Mary's Hospital, The Catholic University of Korea, South Korea. The hMSCs were isolated from bone marrow as previously described [14]. The experiments described here were performed after the fourth cell passage.

Flow cytometry. Flow cytometry (BD FACS Scan, Becton–Dickinson, San Jose, CA) was performed using CD11b, CD29, CD34, CD44, CD45, and Stem cell antigen-1 (Sca-1) cell surface markers to confirm whether the hMSCs maintain their phenotype after expansion in culture [4]. The antibodies used were directed against surface markers CD29, CD34, CD44, and CD45 procured from BD-Bioscience (BD-Bioscience, San Diego, CA), whereas, the Sca-1 antibody was from Pharmingen (Pharmingen, Los Angeles, CA). The samples were incubated with the antibody against each of the surface markers for 30 min which was followed by flow cytometry analysis.

Chemical induction. Primary hMSCs were chemically induced to neuron-like cells in vitro according to the method described by Woodbury et al. [4]. Briefly, subconfluent cultures were preinduced overnight with Dulbecco's modified Eagle's medium (DMEM), 20% fetal bovine serum (FBS), and 10 ng/ml basic fibroblast growth factor (bFGF; Sigma, St. Louis, MO). The preinduction medium was removed, cells were washed with phosphate-buffered saline (PBS) and then changed to serum-free induction medium that consisted of DMEM containing 2% DMSO, 200 μM BHA, 25 mM KCl, 2 mM valporic acid, 10 μM forskolin, 1 μM hydrocortisone and 5 μg/ml insulin (Sigma, St. Louis, MO) [4]. The cells were fixed for immunocytochemistry at 1–24 h post induction.

Time-lapse analysis of the morphological changes during neuronal induction. The hMSCs were grown in 100 mm cell culture Petri dishes, and their images were captured with an inverted differential interference contrast microscope at 200× magnification equipped with a CO_2 and temperature-controlled stage (TE300-Nikon, Minolta, Japan). The cells were maintained at 5% CO_2 at 37 °C for 24 h after changing the cell culture medium to the chemical induction medium containing DMSO/BHA.

Immunocytochemical analysis for neural-specific markers. Immunocytochemistry and confocal microscopy were used to determine the subcellular distribution and organization of the proteins. The hMSCs were fixed in 4% paraformaldehyde in PBS for 10 min followed by permeabilization with 0.5% Triton X-100 in PBS for another 10 min. The specimens were incubated with primary antibodies against Neuron specific enolase (NSE), trkA (Sigma, St. Louis, MO), NF and Nestin (Pharmingen, Los Angeles, CA) overnight at 4 °C, and with FITC- or Rhodamine-conjugated secondary antibody (Molecular Probes Inc., Eugene, OR) for one hour. The nuclear DNA was counterstained with 4′,6′-diamidino-2-phenylindole (DAPI; Sigma, St. Louis, MO). Confocal laser scanning fluorescent microscopy was performed using a 543-nm HeNe laser for excitation and a 565–615 nm filter for emission.

Western blot analysis. The cultured cells were rinsed with PBS and then lysed for 30 min on ice using RIPA-B buffer (0.5% Nonidet P-40, 20 mM Tris, pH 8.0, 50 mM NaCl, 50 mM NaF, 100 μM Na_3VO_4, 1 mM DTT, and 50 μg/ml PMSF). The lysate was centrifuged at 12,000 rpm for 20 min at 4 °C; the pellet was discarded and the supernatant was subjected to SDS–PAGE and Western blot analysis. The blots were blocked in TBS containing 5% BSA and 0.05% Tween 20. The membrane was incubated at 4 °C overnight with the appropriate primary antibodies and then washed extensively in TBS containing 0.05% Tween 20. This was probed with horseradish peroxidase-conjugated anti-rabbit and/or anti-mouse antibodies. Thereafter samples were treated with a secondary antibody (Santa Cruz Biotechnology, Santa Cruz, CA). The blots were subsequently detected by electrochemiluminescence (ECL, Amersham Biosciences, Uppsala, Sweden).

Two-dimensional gel electrophoresis. The cells previously treated with the chemical induction medium and the untreated cells (control group) were suspended in a sample buffer containing 40 mM Tris, 7 M urea, 2 M thiourea, 4% CHAPS, 100 mM 1,4-DTT, and a protease inhibitor cocktail (Complete; Roche, Mannheim, Germany). The suspensions were sonicated for approximately 30 s followed by centrifugation at 100,000 ×*g* for 45 min. The total protein obtained from the chemically induced cells (2 mg), and the untreated cells, was used for electrophoresis. Aliquots of the proteins, in a sample buffer, were applied to nonlinear immobiline dry strips (pH 3–10) (Amersham Biosciences, Uppsala, Sweden). Isoelectric focusing (IEF) was conducted at 80,000 Vh/h. A second dimension was carried out in 9%–16% linear gradient polyacrylamide gels (18 cm × 20 cm × 1.5 mm) at 40 mA per gel at constant current for approximately 5 h, until the dye front reached the bottom of the gel. After protein fixation in 40% methanol and 5% phosphoric acid for 12 h, the gels were stained with Coomassie Blue G250 for 24 h. These gels were destained with double distilled water and scanned in a Bio-Rad G710 densitometer (Bio-Rad, Hercules, CA). The data generated were analyzed using Melanie III software (GenBio, Geneva, Switzerland).

Mass spectrometric analysis. For performing MS fingerprinting, the protein spots were directly cut out of the gels, destained, and treated with trypsin. Aliquots of the peptide mixtures obtained by the trypsinization were applied to a target disk and allowed to air-dry. The spectra were obtained using a Voyager DEPRO MALDI-TOF spectrometer (Applied Biosystems, Foster City, CA). Protein database searches were performed by MS-FIT using monoisotopic peaks. A mass tolerance was first allowed within 50 ppm, and thereafter this was performed at 20 ppm after obtaining the protein list. For all identified proteins, the peptide matching and protein searches were performed against the Swiss-Prot and NCBI databases.

cDNA microarray analysis. All the microarray experiments were done with twin array cDNA chips from Digital Genomics (Seoul, South Korea) as described by Kim et al. [15]. Cy5-labeled RNA from cells responding to chemical induction for 1 h was hybridized together with Cy3-labeled RNA from untreated cells in order to identify the genes, whose expression changed significantly in response to the chemical induction treatment. Four sets of microarray data (from twin arrays and the dye swap) were analyzed with SAM (significance analysis of microarrays) using one-class response format. Genes showing significant changes in expression (>1.0 fold) after chemical induction treatment were selected at a cut off of 5% for the *q* value. The microarray data were analyzed by hierarchic clustering with the BRB ARRAT TOOL Version 3.0 software from the National Cancer Institute.

Microarray data were submitted to the EMBL-EBI (European Bioinformatics Institute; http://www.ebi.ac.uk/miamexpress) for analysis: experiment Accession No., E-MEXP-172; array Accession No., A-MEXP-103.

Electrophysiological recording. The electrophysiological recording of chemically induced cells was performed by growing the cells on a coverslip with a density of 5×10^3 cells/ml and the whole-cell patch clamp method

was used to measure activity of voltage-dependent ion channels. The cells on the coverslip were transferred to the recording chamber and superfused continuously with extracellular solution (1.5–2 ml/min) containing 125 mM NaCl, 2.5 mM KCl, 2 mM $CaCl_2$, 1 mM $MgSO_4$, 1.25 mM KH_2PO_4, 25 mM $NaHCO_3$, and 10 mM D-glucose, bubbled with 95% O_2 and 5% CO_2 (290–295 mOsm). All recordings were performed at 32–33 °C. The patch electrodes (4–6 MΩ) were filled with a pipette solution containing 120 mM K-gluconate, 10 mM KCl, 4 mM MgATP, 10 mM Na_2-phosphocreatine, 0.3 mM Na_3-GTP, 10 mM Hepes, and 50 U/ml creatine phosphokinase (pH 7.25 with KOH). The osmolarity of the pipette solution was 288 mOsm. Cells showing a two or three process was chosen. After obtaining cells in the whole-cell voltage-clamp mode, membrane current was evoked with a 10 mV step increment of command potential for 400 ms from the holding potential of −70 mV.

Statistical analysis. All the numerical data were expressed as means ± standard deviation. The mean average and standard deviation of all of the data were compared among the different groups by using a Kruskal–Wallis *H* test, followed by the Student–Newman–Keuls test for statistical analysis. Statistical significance was defined as $p < 0.05$.

Results

Characterization of hMSCs

The hMSCs characterized using flow cytometer were positive for CD29 (66.1% ± 2.5%), CD44 (99.8% ± 1.1%) and Sca-1 (92.8% ± 1.4%), but they were negative for CD11b, CD34, and CD45. This result shows that the expanded hMSCs maintain their phenotype (Fig. 1).

Morphological changes in chemically induced hMSCs

Contrast microscopy was used to evaluate the morphological changes of the differentiated cells. The untreated and preinduced cultures of hMSCs predominantly consisted of spindle-shaped cells and a few large flat cells (Fig. 2A). Within 3 h, after the addition of induction medium, 73% ± 2.8% of the hMSCs had a changed morphology with neuronal-like phenotypes. These cells were distinguished by highly refractive cell bodies with neuron-like processes terminating in structures that resembled growth cones (Fig. 2B). In these highly refractive cells, the region bound by process tips was reminiscent of the cell shape of untreated hMSCs. Some of the less refractive cells were intermediate in shape between the untreated and neuron-like hMSCs (Fig. 2C, long arrow). These findings suggested that the hMSCs might have differentiated into neuron-like cells. The hMSC derived neurons displayed distinct neuronal morphologies (Fig. 2B), ranging from simple bipolar cells (Fig. 2B and C) to large, extensively branched multipolar cells. However, at 24 h, compared to the cells at 3 h after chemical neuronal induction, the number of attached cells were decreased and the number of floating cells were increased (Fig. 2C).

Immunocytochemistry and Western blot analysis of the neuronal marker genes

To further characterize this chemical neuronal induction phenomenon, immunostaining and Western blotting were performed as explained earlier. The cells that exhibited contracted cell bodies and processes stained dark red for the neuronal specific marker expression (NSE, NF, nestin, and trkA) (Fig. 3E–P), whereas the flat, unresponsive hMSCs remained unstained (Fig. 3A–D). On comparing the results by immunocytochemistry, the percentage of cells positively reactive for NSE, NF, nestin and trkA at 3 h was 74.8% ± 2.5%, NF 79.2% ± 2.3%, 31.6% ± 3.8%, and 55.6% ± 2.4%, respectively, and the percentage of cells positively reactive for these markers at 24 h was 60.6% ± 2.5%, 78.2% ± 2.3%, 20.2% ± 3.8%, and 42.6% ± 2.4%, respectively (Fig. 3M–P). These results indicated that there was statistical decrease in the percentage of intensity for NSE, nestin, and trkA ($p < 0.05$) whereas no statistical decrease was observed for NF. Western blotting of the untreated hMSCs was performed using the same antibodies and β-actin as internal control (Fig. 4) resulted in low expression levels of neuronal specific markers (NSE, NF, nestin, and trkA). Western blotting was performed to confirm the

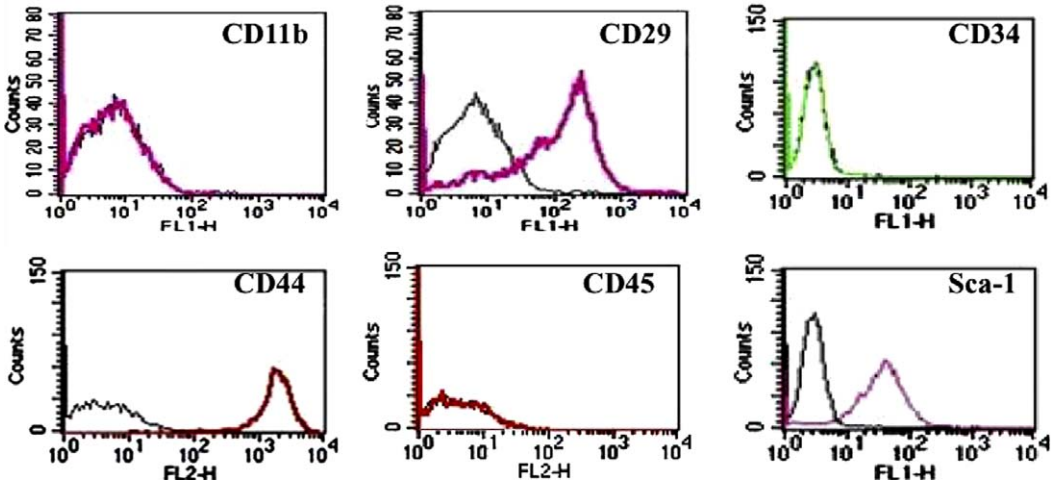

Fig. 1. Flow cytometry analysis of hMSCs after staining with FITC-conjugated CD11b, CD34, CD45, Sca1, CD29, and CD44 antibodies: CD29— 66.1% ± 2.5%, CD44— 99.8% ± 1.1%, and Sca-1— 92.8% ± 1.4%.

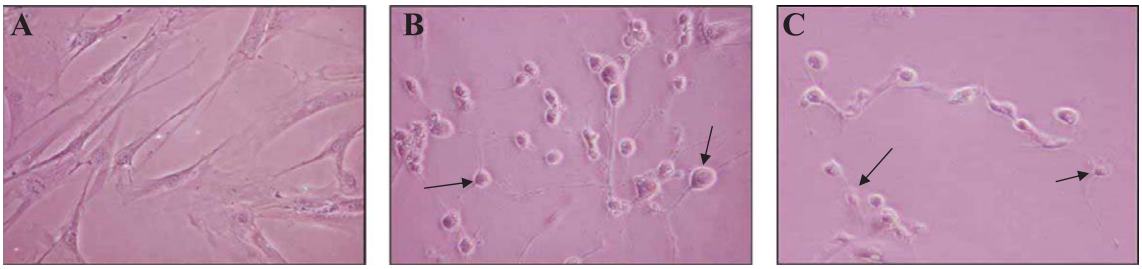

Fig. 2. The hMSCs were kept as an untreated control (A) or they were treated with chemical induction media (B,C) up to 24 h. The phase contrast images were collected at different time points (3 and 24 h). The arrows in B,C indicate the "neuron-like structure" in the cells. The untreated cultures of hMSCs consisted predominantly of spindle-shaped cells and a few large, flat cells. At 3 h after the addition of induction medium, 73% of the hMSCs had changed their morphology and had adopted neuronal-like phenotypes. At 24 h, the number of attached cells decreased and the number of floating cells increased. The images are representative of three experiments (200 ×).

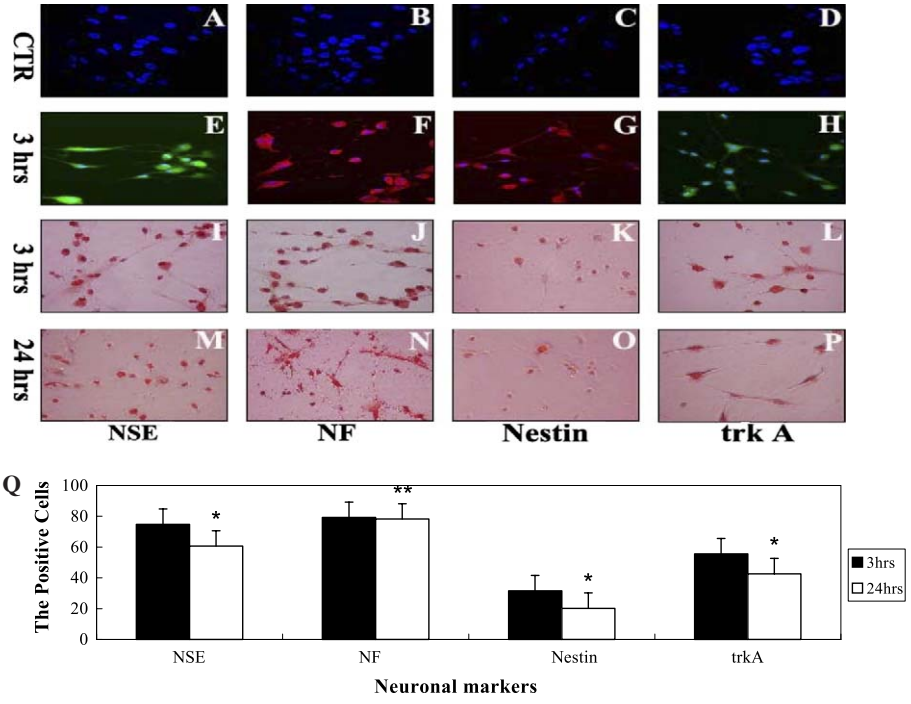

Fig. 3. The hMSCs were kept as a control (A–D) or they were treated with chemical induction medium (E–P) for 3 or 24 h, and they were stained with neuron specific enolase (NSE), neurofilament (NF), and nestin and TrkA antibody (immunofluorescence). Comparisons of samples at 3 and 24 h after immunocytochemistry; the percentage of positive cells reactive to NSE, NF, nestin, and trkA at 3 h was NSE (74.8% ± 2.5%), NF (79.2% ± 2.3%), nestin (31.6% ± 3.8%), and trkA (55.6% ± 2.4%). However, the percentage of positive cells reactive to NSE, NF, nestin, and trkA at 24 h was NSE (60.6% ± 2.5%), NF (78.2% ± 2.3%), nestin, (20.2% ± 3.8%) and trkA (42.6% ± 2.4%) (M–P). The data represent means SEM of staining expression intensity ($^{*}p < 0.05$ vs 3 h; $^{**}p < 0.01$ vs 3 h). The images represent three experiments (A–H 400×, I–P 200×).

specificity of the immunocytochemical results for these markers which showed a marked correlation at 3 h ($p > 0.05$) and statistically insignificant results at 24 h, respectively, on comparing the band densities at 3 and 24 h. The correlation of Western blotting results with the immunocytochemical results suggests that chemical induction may differentiate hMSCs into a neuronal cell lineage.

Two-dimensional gel electrophoresis profile

To confirm the neuronal differentiation of hMSCs, we used a proteomic approach. A representative two-dimensional gel image of the protein lysates from the hMSCs with and without the chemical induction medium treatment is shown in Fig. 5. About 1000 protein spots were resolved and identified with high confidence (>95%). Overall, eighty protein spots were found consistently up-regulated or down-regulated by more than twofold after chemical induction medium treatment for 3 h. Twenty protein spots were successfully identified with high confidence with in-gel trypsin digestion followed by tandem mass spectrometry. The proteins identified were grouped according to their primary functions as listed in Table 1. The majority of these spots have an *n*-fold value either larger than two or smaller than 0.5. Cytoskeleton proteins (vimentin, γ-actin), metabolic enzymes (glyceraldehyde-3-phosphate dehydrogenase),

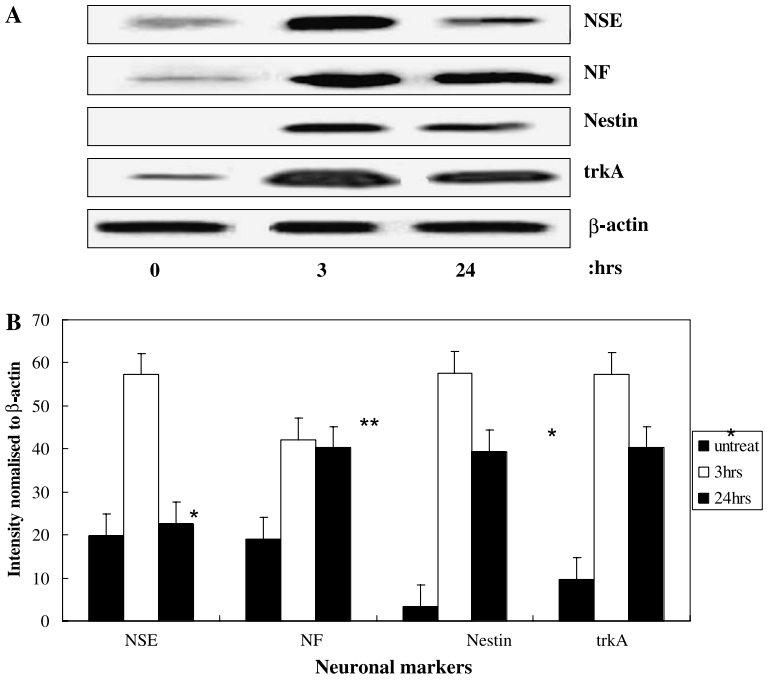

Fig. 4. The hMSCs were treated with chemical induction media for 3 or 24 h, and the protein expression was analyzed by Western blotting. The β-actin bands show an equal loading of proteins for each sample. The data represent means SEM of the staining expression intensity ($^{*}p < 0.05$ vs 3 h; $^{**}p < 0.01$ vs 3 h).

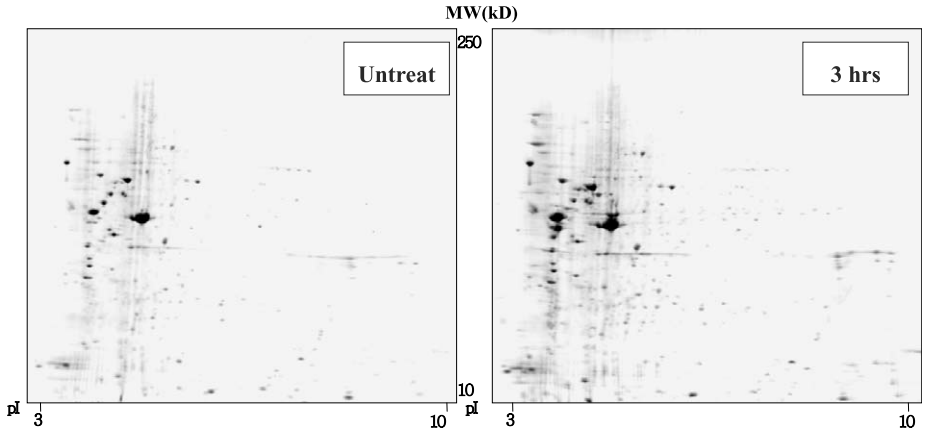

Fig. 5. The hMSCs were either kept as a control (no treatment) or they were treated with chemical induction media for 3 h. The proteins from the hMSCs were extracted and separated on nonlinear immobiline dry strips (pH 3–10) and were run through 9–16% SDS-PAGE gel. The gel was stained with Coomassie blue G-250. The protein spots were analyzed by MALDI-TOF.

transcription/translational regulation protein, assembly proteins (Annexin A2), ribosomal protein, and inflammatory/stress responsive proteins (BiP protein) were also observed. These results showed increase in the intermediate filament vimentin after neuronal induction of the hMSCs. The specificity of the results obtained was confirmed by Western blotting as shown in Fig. 6B.

Microarray analysis

To confirm whether these chemically induced cells were real neurons, we used DNA microarray analysis to profile chemically -induced gene expression. We found 8180 gene differences on comparing the untreated and chemically induced cells. Among these, 27 genes were found to be two-fold up- or down-regulated. These 27 genes were divided into eight functional categories as depicted in Table 2. We expected an up-regulation, in the gene expression, by the neurons. However Fibroblast growth factor 7, Caldesmon 1, Rho family GTPase 3, and potassium channel tetramerization genes related to the neurons showed a double fold decrease.

Effect of chemical induction treatment on voltage-dependent membrane current

Voltage-dependent ion channel activity was measured to investigate the effects of chemical medium treatment on the

Table 1
Proteins identified in two-dimensional electrophoresis gel

Protein identified	Accession No.	Mass (kDa)/p*I*	% C[a]
Increased protein			
BiP protein	AAF13604	71.03/5.2	16
Nebulin	AAB02622	350.3/9.2	7
Vimentin	AAA61279	53.75/5.0	13
γ- Actin	JC5818	41.99/5.3	49
FK506-binding protein	AAD40379	25.92/6.0	27
Vimentin	NP003371	53.72/5.1	29
Annexin A2	AAH09564	38.83/7.7	50
Glyceraldehyde-3-phosphate dehydrogenase	CAA25833	Unknown/8.26	20
Bamacan homolog	AAD32447	78.83/5.8	15
UCRI_UMAN ; RIESKE IRON - SURFUR PROTEIN : RISP	AAD38242	29.94/8.9	16
Ribosomal protein	AAB00969	21.83/10.1	18
Hypothetical protein	CAD97642	47.42/7.7	32
Decreased protein			
Lamin A/C isoform 2	NP005563	65.17/6.4	30
Lamin A/C isoform 2	NP005563	65.17/6.4	38
Septin 11	NP060710	Unknown/6.36	25
Serine (or cysteine) proteinase inhibitor, clade H	NP001226	46.54/8.9	32
γ-Actin	AAA51580	26.15/5.6	32
ACTB protein	AAH12854	40.54/5.6	33
ACTB protein	AAH12854	40.54/5.6	33
Manganese-containing superoxide dismutase	AAP34407	23.65/6.9	29

The hMSCs were either kept as an untreated control or they were treated with chemical induction medium for 3 h. The resulting peptides were used for LC–MS/MS analysis, and the proteins were identified by searching the databases with using peptide sequences.
[a] Sequence coverage.

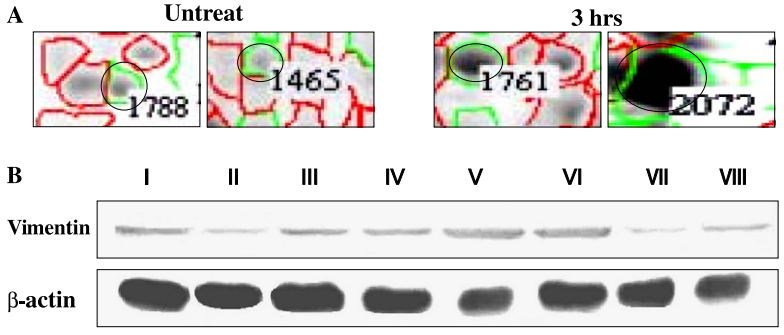

Fig. 6. (A) Identification of vimentin in the two-dimensional gels. The hMSCs were kept as a control or they were treated with chemical induction media for a time course and cell lysates were subjected to two-dimensional electrophoresis and Coomassie blue G-250 staining. Spots 1465 and 1788 showed increase after chemical induction media treatment and these were identified as vimentin. (B) Protein expression of vimentin in response to chemical induction media. The hMSCs were treated with chemical induction media for preinduction for 1, 3, 5, 8, 12, and 24 h, and the protein expression was analyzed by immunoblotting. The β-actin bands show equal loading of the proteins in each sample Expression. (I, untreat control; II, preinduction; III, 1 h induction; IV, 3 h induction; V, 5 h induction; VI, 8 h induction; VII, 12 h induction; and VIII, 24 h induction).

hMSCs. The treated cells showed small outward currents with a depolarizing voltage step from a holding potential of −70 mV (Fig. 7). However, no apparent voltage-dependent inward current was seen.

Discussion

Bone marrow stromal stem cells have shown to possess the potential to differentiate into a variety of mesenchymal stem cells such as adipocytes, chondrocytes, myocytes, and non-mesenchymal lineage neurons [1–3]. The properties of multipotent progenitor cells make them an attractive target for use in therapeutic and bioengineering applications [16,17]. The ability of MSCs to differentiate in vitro towards a neural lineage allows potential therapeutic applications for the treatment of neurological diseases and CNS trauma.

Woodbury et al. reported that MSCs undergo rapid transformation into cells with neuron-like phenotypes following treatment with a chemical induction medium containing DMSO [4,10]. However, Neuhuber et al. reported the formation of neurite-like processes following chemical induction, as a result of cytoplasm retraction caused by β-actin depolymerization and not by microtubule-mediated

Table 2
Differential gene expression for chemical induction and untreated cells by microarray analysis

Gene name	Gene symbol	Accession	Cytoband	Log2 ratio
Upregulation				
Histone 1, H2ae	HIST1H2AE	AA436989	6p22.2-p21.1	1.08
Heme oxygenase (decycling) 1	HMOX1	NM_002133	22q12	1.09
Ectonucleotide pyrophosphatase/phosphodiesterase 1	ENPP1	M57736	6q22-q23	1.09
Thymidylate synthetase	TYMS	X02308	18p11.32	1.11
Nucleoside phosphorylase	NP	AA311617	14q13.1	1.29
Asparagine synthetase	ASNS	NM_001673	7q21.3	1.35
Metallothionein 1F (functional)	MT1F	AI814448	16q13	1.39
Histone 2, H2be	HIST2H2BE	NM_003528	1q21-q23	1.74
Downregulation				
Leptin receptor	LEPR	U52914	1p31	−2.37
Cysteine-rich, angiogenic inducer, 61	CYR61	Y12084	1p31-p22	−1.99
Fibroblast growth factor 7 (keratinocyte growth factor)	FGF7	AI075338	15q15-q21.1	−1.95
Interleukin 8	IL8	Y00787	4q13-q21	−1.80
Immediate early response 3	IER3	AI185199	6p21.3	−1.65
Superoxide dismutase 2, mitochondrial	SOD2	Y00472	6q25.3	−1.53
Matrix metalloproteinase 11 (stromelysin 3)	MMP11	X57766	22q11.2	−1.30
Thrombospondin 2	THBS2	L12350	6q27	−1.24
Rho family GTPase 3	ARHE	W03441	2q23.3	−1.21
Thrombospondin 4	THBS4	Z19585	5q13	−1.20
Hypoxia-inducible factor 1, alpha subunit	HIF1A	U29165	14q21-q24	−1.10
Connective tissue growth factor	CTGF	X78947	6q23.1	−1.09
Dual specificity phosphatase 6	DUSP6	NM_001946	12q22-q23	−1.07
Caldesmon 1	CALD1	M83216	7q33	−1.06
Cyclin A1	CCNA1	U66838	13q12.3-q13	−1.06
Potassium channel tetramerisation domain containing 12	KCTD12	AA402981	13q22.3	−1.06
BRCA1 associated protein	BRAP	AF035620	12q24	−1.05
Immediate early response 3	IER3	AI185199	6p21.3	−1.65
Matrix Gla protein	MGP	AA484893	12p13.1-p12.3	−1.01

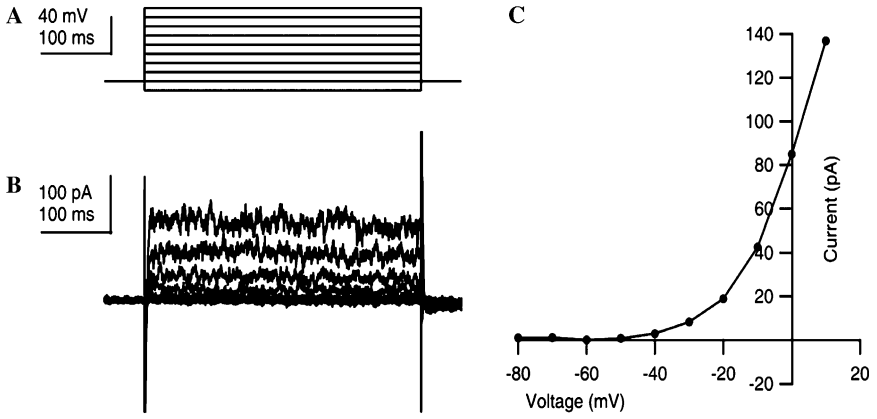

Fig. 7. Whole-cell current was evoked by a depolarizing voltage step for 400 ms from −80 to 10 mV after holding at −70 mV. (A) Voltage command used. (B) Total membrane current evoked. (C) Voltage–current plot from (B). Current was measured from 100 to 300 ms after applying the command potential.

extension. They also demonstrated that the treatment of bone marrow cells with different combinations of growth factors and retinoic acid (RA) induced a neuronal phenotype however; the intracellular distribution of neural proteins was distinct from that of genuine neurons [8]. Thus, the extent to which MSCs may be able to differentiate into mature, functional neurons remains unknown. One of the studies postulated that the morphological and immunocytochemical changes of hMSCs, following treatment with a "neuronal induction and differentiation" medium, were not the result of genuine neuronal differentiation, but rather the changes represent cellular responses to chemical stress [9].

These observations led us to reconsider and study whether true neuronal differentiation of hMSCs takes place following treatment with the chemical induction medium. For confirming the neuronal differentiation of hMSCs a proteomics approach was used.

The hMSCs used in this study were positive for CD 29 (66.1% ± 2.5%), CD 44 (99.8% ± 1.0%), and Sca-1

(92.8% ± 1.4%), indicating that hMSCs retain the capacity to differentiate into mesenchymal and non-mesenchymal derivatives, and these adult cells are capable of self-renewing and exhibit multipotency, thereby fulfilling the criteria for a stem cell population. The characteristic features of neurons include bipolar or extensively branched multipolar cells with neuronal growth cones that are motile and extend along processes and at their tips [8]. Our observations revealed that within 3 h of treatment with the induction medium, three-fourths of the hMSCs had a changed morphology and adopted neuronal-like phenotypes. This phenotype was distinguished by highly refractive cell bodies with neurite-like processes that terminated in structures resembling growth cones (Fig. 2B). These findings suggested that the hMSCs might have differentiated to neuron-like cells. However, the observations with time-lapse microscopy demonstrated that these differentiated hMSCs shrank rapidly (within minutes) in response to the "chemical induction medium" leaving behind the neuron-like processes. These cells failed to grow new extensions at 24 h after neuronal differentiation. These findings suggested that the neuron-like morphology might have been caused by the retraction of cytoplasm rather than by an active process of microtubule-mediated extension [8].

To confirm neuronal differentiation, specific neuronal makers including: NSE, NF, nestin, and trkA were used. Woodbury et al. had demonstrated that NSE was expressed in the early stage of neuronal differentiation using chemical induction medium [4], we have also observed similar results at 3 h, however this decreased with time as demonstrated by immunocytochemistry and Western blotting results.

Woodbury et al. [4] reported that trkA was expressed less in the early stages of neuronal differentiation, which increases at the later stages. In contrast to our studies which show that trkA was expressed more in the early stages compared to the later stages of neuronal differentiation following "chemical induction." This discrepancy may be due to the fact that we conducted our studies on human MSC, not on rodent MSC as reported by Woodbury. Though the neuronal chemical induction media induced a strong expression of neuronal markers such as NSE, NF, nestin, and trkA at 3 h, the intensity of the neuronal marker expression was significantly reduced at 24 h, except for NF. Western blotting with neuronal markers indicated that labeling intensity of the chemically induced hMSCs increased for some neuronal markers at 3 h compared with non-induced cells. We suggest that these findings may be due to an increase in the antigen per unit area, which may be the result after cell shrinkage and retraction of cellular processes [9].

Recent studies have indicated that both neural induction and neuronal differentiation appear to be connected to the cell cycle control system, which regulates the maintenance, proliferation, specification, and differentiation of neural stem cells and neuronal precursors [18,19]. The time-lapse imaging of both Woodbury et al. and Paul et al. showed that the induced MSCs dramatically contracted and changed their morphology compared to neuron-like cells not undergoing cell division [4,9]. This finding is supported by a subsequent study from the same group demonstrated that MSCs can directly differentiate into neurons without passing through a mitotic stage [20].

Our findings do not rule out the possibility that hMSCs can differentiate into neurons. However, in order to avoid any discrepancies in the in vitro differentiation experiments we performed proteomic analysis to assess the types of proteins that were changed during the chemical neuronal induction of the hMSC. Large-scale proteome screening was done to identify unique markers and elucidate interconnections between the different cellular signaling pathways. We have for the first time profiled the global protein expression in hMSCs after chemical induction stimulation.

Neuronal development is a complex process that involves several successive steps and signaling events [21]. During neural induction, bone morphogenetic protein (BMP) antagonism has been viewed as the central and initiating event in neural induction. According to this theory, neural specification occurs as a default pathway when BMP signaling is blocked by inhibitors like Noggin or Chordin, Candidate positive inducers have recently been isolated that belong to Wnt, fibroblast growth factor (FGF), and insulin-like growth factor (IGF) families [18]. Therefore, we tried to determine whether there was increase or decrease in neuronal signaling factors, as well as neuronal markers such as NSE, NF, nestin, and trkA, via a proteomics analysis.

We could predict an increase in the Wnt, fibroblast growth factor (FGF), insulin-like growth factor (IGF) families, Noggin, Chordin, and the neuronal makers [18,22], and decrease in the BMP families. Because there was a marked increase in the neuronal markers compared to the control group, we performed the proteomic analysis after 3 h of chemical neuronal induction; however, there was no increase or decrease in the mentioned genes, as depicted in Table 1. We found an increase in cytoskeleton proteins (vimentin, γ-actin), metabolic enzymes (glyceraldehyde-3-phosphate dehydrogenase), transcription/translational regulation protein assembly proteins (Annexin A2), miscellaneous (hypothetical protein, ribosomal protein), and inflammatory/stress responsive proteins (BiP protein). From the proteomics results, our findings suggest that the chemically induced neuronal media simply change the shape of the hMSCs to neuron-like pseudo-neurons instead of inducing the development of genuine neurons.

Another significant finding, from our study, was that the chemical induction medium coordinates the expression of vimentin to promote the differentiation of hMSCs. We could identify the protein vimentin in the stem cells, which is the most ubiquitous intermediate filament protein. In hMSCs, vimentin is replaced by other intermediate filament proteins during differentiation, cellular proliferation,

and apoptosis. Our study also suggests that there might be increase in vimentin, instead of neuronal markers, after chemical induction which may change the morphology of the hMSCs after chemical neuronal induction.

We anticipated an increase in these neuron related genes using DNA microarray analysis. However, we found a double fold decrease in their levels. Results of the proteomics and DNA microarray analysis revealed that the chemically induced neuronal cells did not show features consistent with a genuine neuron. To further reconfirm our results, we performed the patch clamp test and synapsin staining of these chemically induced cells. These results showed no resemblance of the chemically induced cells to true neurons.

The present study indicated that the morphological, immunocytochemical, and Western blot changes observed in hMSCs following treatment with a ''neuronal induction and differentiation'' medium are not the result of genuine neuronal differentiation, but rather represent cellular responses to chemical stress. We suggest that confirmation of genuine neuronal differentiation of hMSCs would require not only the adoption of a neuronal morphology and gene expression but also the acquisition of the electrophysiological properties and genetic expression of true neurons as reported earlier [9]. In addition, the differentiated cells should be maintained and confirmed as genuine neurons after prolonged culture with growth factors like human epidermal growth factor (hEGF), basic fibroblast growth factor (bFGF), fibroblast growth factor-8 (FGF-8), and brain-derived neurotrophic factor (BDNF) [23].

Acknowledgments

This study was supported in part by a grant of the Korea Health 21 R&D Project, Ministry of Health and Welfare, Republic of Korea (03-PJ10-PG6-GP01-0002) and by a grant of the Korea Health 21 R&D Project, Ministry of Health Welfare, Republic of Korea (00-PJ3-PG6-GN02-0002).

References

[1] J. Sanchez-Ramos Song, S.M. Dailey, F. Cardozo-Pelaez, C. Hazzi, T. Stedeford, A. Willing, T.B. Freeman, S. Saporta, T. Zigova, P.R. Sanberg, E.Y. Snyder, The X-gal caution in neural transplantation studies, Cell Transpl. 9 (2000) 657–667.

[2] Y. Jiang, B.N. Jahagirdar, R.L. Reinhardt, R.E. Schwartz, C.D. Keene, X.R. Ortiz-Gonzalez, M. Reyes, T. Lenvik, T. Lund, M. Blackstad, J. Du, S. Aldrich, A. Lisberg, W.C. Low, D.A. Largaespada, C.M. Verfaillie, Pluripotency of mesenchymal stem cells derived from adult marrow, Nature 418 (2002) 41–49.

[3] P. Kabos, M. Ehtesham, A. Kabosova, K.L. Black, J.S. Yu, Generation of neural progenitor cells from whole adult bone marrow, Exp. Neurol. 178 (2002) 288–293.

[4] D. Woodbury, E.J. Schwarz, D.J. Prockop, I.B. Black, Adult rat and human bone marrow stromal cells differentiate into neurons, J. Neurosci. Res. 61 (2000) 364–370.

[5] S.C. Hung, H. Cheng, C.Y. Pan, M.J. Tsai, L.S. Kao, H.L. Ma, In vitro differentiation of size-sieved stem cells into electrically active neural cells, Stem Cells 20 (2002) 522–529.

[6] K.M. Safford, K.C. Hicok, S.D. Safford, Y.D. Halvorsen, W.O. Wilkison, J.M. Gimble, H.E. Rice, Neurogenic differentiation of murine and human adipose-derived stromal cells, Biochem. Biophys. Res. Commun. 294 (2002) 371–379.

[7] M. Romero-Ramos, P. Vourc'h, H.E. Young, P.A. Lucas, Y. Wu, O. Chivatakarn, R. Zaman, N. Dunkelman, M.A. el-Kalay, M.F. Chesselet, Neuronal differentiation of stem cells isolated from adult muscle, J. Neurosci. Res. 69 (2002) 894–907.

[8] B. Neuhuber, G. Gallo, L. Howard, L. Kostura, A. Mackay, I. Fischer, Re-evaluation of in vitro differentiation protocols for bone marrow stromal cells: disruption of actin cytoskeleton induces rapid morphological changes and mimics neuronal phenotype, J. Neurosci. Res. 77 (2004) 192–204.

[9] P. Lu, A. Blesch, M.H. Tuszynski, Induction of bone marrow stromal cells to neurons: differentiation, transdifferentiation, or artifact? J. Neurosci. Res. 77 (2004) 174–191.

[10] D. Woodbury, K. Reynolds, I.B. Black, Adult bone marrow stromal stem cells express germline, ectodermal, endodermal, and mesodermal genes prior to neurogenesis, J. Neurosci. Res. 69 (2002) 908–917.

[11] D. Wang, J.S. Park, J.S. Chu, A. Krakowski, K. Luo, D.J. Chen, S. Li, Proteomic profiling of bone marrow mesenchymal stem cells upon transforming growth factor beta1 stimulation, J. Biol. Chem. 279 (2004) 43725–43734.

[12] S.D. Patterson, R.H. Aebersold, Proteomics: the first decade and beyond, Nat. Genet. 33 (2003) 311–323.

[13] T. Rabilloud, Two-dimensional gel electrophoresis in proteomics: old, old fashioned, but it still climbs up the mountains, Proteomics 2 (2002) 3–10.

[14] N. Jaiswal, S.E. Haynesworth, A.I. Caplan, S.P. Bruder, Osteogenic differentiation of purified, culture-expanded human mesenchymal stem cells in vitro, J. Cell. Biochem. 64 (1997) 295–312.

[15] T.W. Kim, Y.J. Kwon, J.M. Kim, Y.H. Song, S.N. Kim, Y.J. Kim, MED16 and MED23 of Mediator are coactivators of lipopolysaccharide- and heat-shock-induced transcriptional activators, Proc. Natl. Acad. Sci. USA 101 (2004) 12153–12158.

[16] K. Shindo, N. Kawashima, K. Sakamoto, A. Yamaguchi, A. Umezawa, M. Takagi, K. Katsube, H. Suda, Osteogenic differentiation of the mesenchymal progenitor cells, Kusa is suppressed by Notch signaling, Exp. Cell Res. 290 (2003) 370–380.

[17] P. Bianco, M. Riminucci, S. Gronthos, P.G. Robey, Bone marrow stromal stem cells: nature, biology, and potential applications, Stem Cells 19 (2001) 180–192.

[18] L. Bally-Cuif, M. Hammerschmidt, Induction and patterning of neuronal development, and its connection to cell cycle control, Curr. Opin. Neurobiol. 13 (2003) 16–25.

[19] F. Cremisi, A. Philpott, S. Ohnuma, Cell cycle and cell fate interactions in neural development, Curr. Opin. Neurobiol. 13 (2003) 26–33.

[20] G. Munoz-Elias, D. Woodbury, I.B. Black, Marrow stromal cells, mitosis, and neuronal differentiation: stem cell and precursor functions, Stem Cells 21 (2003) 437–448.

[21] S.I. Wilson, T. Edlund, Neural induction: toward a unifying mechanism, Nat. Neurosci. 4 (2001) 1161–1168.

[22] J. Kohyama, H. Abe, T. Shimazaki, A. Koizumi, K. Nakashima, S. Gojo, T. Taga, H. Okano, J. Hata, A. Umezawa, Brain from bone: efficient ''meta-differentiation'' of marrow stroma-derived mature osteoblasts to neurons with Noggin or a demethylating agent, Differentiation. 68 (2001) 235–244.

[23] X. Long, M. Olszewski, W. Huang, M. Kletzel, Neural cell differentiation in vitro from adult human bone marrow mesenchymal stem cells, Stem Cells Dev. 14 (2005) 65–69.